Available on CMS information server

CMS NOTE 2003/015

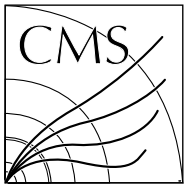

The Compact Muon Solenoid Experiment

CMS Note

Mailing address: CMS CERN, CH-1211 GENEVA 23, Switzerland

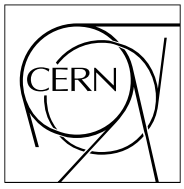

The Silicon Sensors for the Compact Muon Solenoid Tracker - Design and Qualification Procedure

J.-L. Agram[1)], M. M. Angarano[2)], S. Assouak[3)], T. Bergauer[4)], G. M. Bilei[5)], L. Borrello[6)], M. Brianzi[7)], C. Civinini[7)], A. Dierlamm[8)], N. Dinu[2)], N. Demaria[9)], L. Feld[5)], E. Focardi[7)], J.-C. Fontaine[1)], E. Forton[3)], A. Furgeri[8)], Gh. Gregoire[3)], F. Hartmann[8)], A. Honma[5)], P. Juillot[10)], D. Kartashov[6)], M. Krammer[4)], A. Macchiolo[7)], M. Mannelli[5)], A. Messineo[6)], E. Migliore[9)], O. Militaru[6,a)], C. Piasecki[8)], R. Santinelli[2)], D. Sentenac[6)], L. Servoli[2)], A. Starodumov[6)], G. Tonelli[6)], J. Wang[6,b)]

Abstract

The Compact Muon Solenoid (CMS) is one of the experiments at the Large Hadron Collider (LHC) under construction at CERN. Its inner tracking system consist of the world largest Silicon Strip Tracker (SST). In total it implements 24244 silicon sensors covering an area of 206 m^2. To construct a large system of this size and ensure its functionality for the full lifetime of ten years under LHC condition, the CMS collaboration developed an elaborate design and a detailed quality assurance program. This paper describes the strategy and shows first results on sensor qualification.

[1)] Groupe de Recherches en Physique des Hautes Energies, UHA Mulhouse, France

[2)] INFN-Perugia and University of Perugia, Perugia, Italy

[3)] Institute of Physics, University of Louvain, Louvain-la-Neuve, Belgium

[4)] Institute for High Energy Physics, Austrian Academie of Sciences, Vienna, Austria

[5)] CERN, European Laboratory for Particle Physics, Geneva, Switzerland

[6)] INFN-Pisa and University of Pisa, Pisa, Italy

[7)] INFN-Florence and University of Florence, Florence, Italy

[8)] Institut für Experimentelle Kernphysik, University of Karlsruhe, Germany

[9)] INFN-Torino and University of Torino, Torino, Italy

[10)] Institut de Recherches Subatomiques, ULP/CNRS, Strasbourg, France

[a)] on leave from NIPNE-HH, Bucharest, Romania

[b)] on leave from Institute of Modern Physics Chinese Academy of Sciences ,Lanzhou, P.R.China

1 Introduction

1.1 Tracker Layout

The CMS tracker consists of ten barrel layers, plus two set of nine endcap disks, altogether covering a pseudorapidity range of $|\eta| \leq 2.5$. The layout is shown in Fig. 1. Four inner barrel layers (TIB) are assembled in shells complemented by two inner endcaps each composed of three small disks (TID). The outer barrel structure (TOB) consists of six concentric layers closing the tracker towards the calorimeter. The endcap modules (TEC) are mounted in seven rings on nine disks per each side consisting of sectors, each covering 1/16 of a full disk.

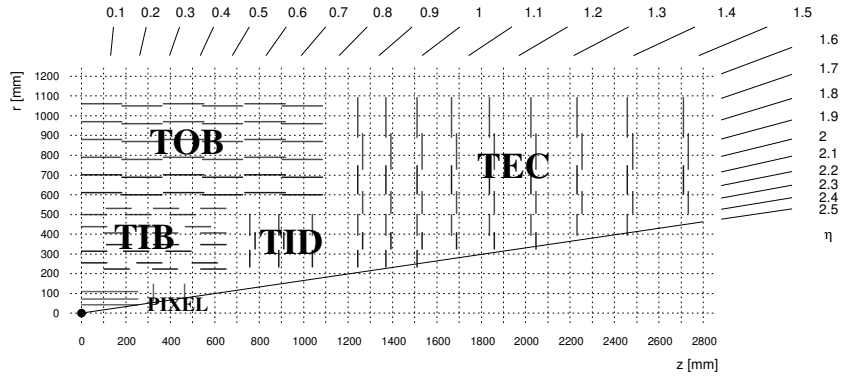

Figure 1: One quarter longitudinal view of the CMS Silicon Tracker Layout

The inner four barrel and four innermost rings of the forward detector are composed of silicon sensors of 320 μm thickness, while the outer six barrel layers and the three outermost rings of the endcaps are designed to house sensors of 500 μm thickness. All thin silicon wafers will be fabricated using silicon of relatively low resistivity (1.5 - 3.0 kΩ cm) whereas the 'thick' wafers will be made of silicon with high resistivity (3.5 - 7.5 kΩ cm). Each detection unit in the inner region (TIB, TID and the first four ring of TEC) is composed of a single micro-strip sensor, with two daisy-chained sensors in the outer region (TOB and the last three rings of TEC). The first two layers in TIB and TOB, the first two rings in TID and rings 1, 2, 5 in TEC are instrumented with double-sided modules. These are made with two independent single-sided detection units, mounted back to back, with the second one being rotated by 100 mrad with respect to the first.

A pixel vertex detector will be mounted further inside of the strip detector. The complete tracking volume will rest in an inert Nitrogen atmosphere at -10°C to avoid the effects of reverse annealing.

1.2 The Quality Assurance Scheme

The large number of sensors forces CMS to develop a quality assurance procedure to ensure the full compliance of all delivered sensors with the technical specifications. Fig. 2 shows the sensor flow during production between the laboratories involved. The contracts for the procurement of the silicon sensors contains a comprehensive list of tests to be performed and the correspondingly specified acceptance criteria to be checked by the companies. It is the goal of these tests to ensure that at least 99% of the delivered sensors will later pass the CMS quality tests.

After receiving and registrating sensors at CERN, the sensors and the corresponding test structures are shipped to the 'Quality Test Centers' (QTC see section 3). These four centers are responsible for the overall quality. In these QTC centres samples of sensors are fully characterised. A given percentage of the test structures and some sensors will be distributed to the 'Process Qualification Centers' (PQC see section 4) were several parameters related to the production process are measured and long-term tests are done. Further test structures and sensors are sent to the 'Irradiation Qualification Centers' (IQC see section 5). In the IQC centres test structures and sensors are irradiated with neutrons or protons. The adhesion of wire bonds is also checked using test structures at the laboratories responsible for module bonding.

2 Design of Sensors and Test Structures

Both the 500 μm thick silicon sensors and the 320 μm thick sensors will be manufactured using 6" technology, with the standard planar process usually employed in the IC industry. One single detector is produced from each wafer and it is requested to lie inside a fiducial circle of about 13.5 cm diameter. The wafer thickness must be

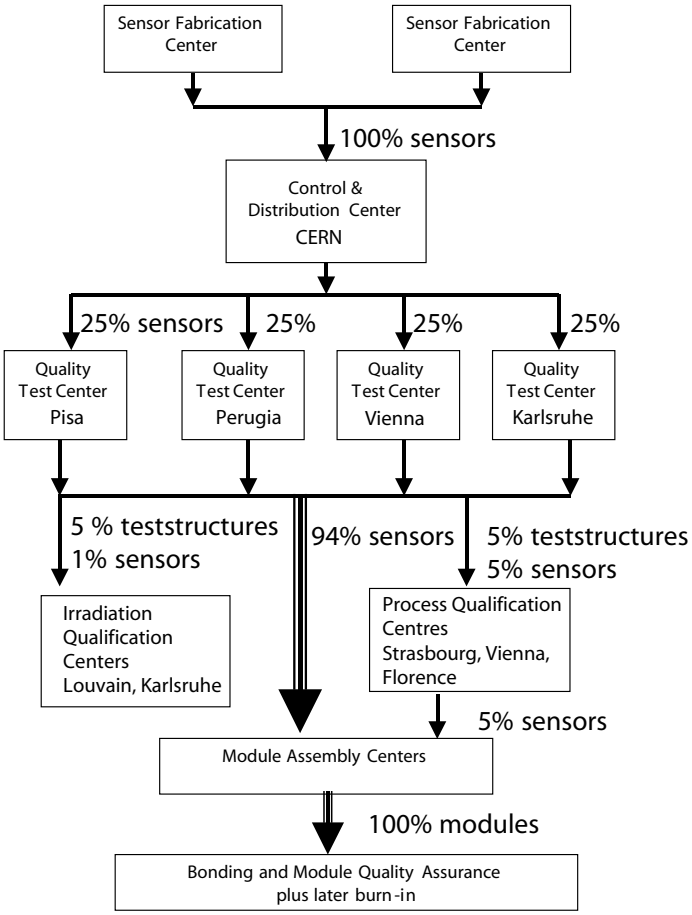

Figure 2: Logistics of the CMS Quality Assurance and Production. A reasonable large percentage of sensors will be continuously checked during the full production with respect to the aspects of quality, process stability, bondability and radiation hardness.

within 20 μm of the specification, the flatness such that the wafer warp is less than 100 μm, the dicing accuracy at the level of 20 μm. The mask alignment tolerance is 1 μm, as is the requested precision of the implants dimensions. The producers are requested to supply sensors polished in the front and acid etched in the back side.

The main strategies of CMS to ensure the radiation hardness of the silicon sensors consist of reducing the surface damage, delaying the bulk type inversion and using stable sensors with respect to high voltage. CMS will use silicon with $\langle 100 \rangle$ lattice orientation which has fewer dangling bonds than standard $\langle 111 \rangle$ silicon. This leads to a suppression of surface damage resulting in reduced increase of interstrip capacitance, i.e. capacitive noise after irradiation, which is the main noise contribution at working temperature of -10^{o}C. Implementation of a metal overhang over the p^+ strip (improved field configuration) results in a more stable detector with respect to high bias voltages of up to 500 V. Using low resistivity silicon delays the inversion point in time resulting in a lower depletion voltage after ten years of LHC operation. An overview of radiation hardening features implemented in the CMS sensors are summarized in [1].

An uniform, metallized, n^+ layer is present on the sensor backside providing an ohmic contact between the bulk and the metal contact. Moreover, the presence of this highly doped n^+ layer acts as a barrier for minority carriers coming from the depleted bulk and for majority carriers injected from the metal contacts, keeping the overall leakage current very low. In addition, on the junction side, an n^+ implant is required along the edges of the device, in order to prevent the space charge region from reaching the cutting edge, thus protecting the active area from injection of charges originating in this heavily damaged region.
The distance of the implanted region from the cutting edge, twice the thickness plus 110 μm, minimizes the occurrence of breakdown phenomena. The active region is surrounded by two p^+ rings. The external one prevents the flowing of leakage current from the sensor edges to the internal ring, used to bias the strips. The metal field plates extend beyond the implantation, to avoid high fields at its edge. The very large metal over-hang on the guard ring external side acts as a multi-guard structure, allowing electric field smoothing. Also the ring geometry, with

rounded corners, helps to avoid discharges while operating the device at high voltage.

The passivation of the front side improves the detector stability and reduces the handling fragility.

2.1 Sensors

p^+ implantations are performed on the front side of the sensor in order to define the strip shaped diodes. The width of the implant strips depends on the strip pitch; a constant width/pitch ratio of 0.25 is used. This value is a compromise between an high width/pitch ratio that reduces the field peak located at the p^+ edge and a low value that reduces the total strip capacitance. Aluminum read-out strips, capacitatively coupled over the p^+-implants, are 15 % wider than the width of the implant underneath. The overhang ranges from 4 to 8 μm, depending on the strip pitch. As in the case of the bias and guard rings, this design choice moves the high edge electric field from the silicon into the much more resistant oxide layer, reducing the risk of electrical breakdown. The thickness of the metal layer is required to be greater than 1.2 μm to limit the noise contribution due to the resistance of the electrode.
An array of polysilicon resistors is used to bias the implant strips. These resistors are aligned and connected to each strip from the bias ring, on the same side of the sensor, where a metallised probe pad (DC pad), contacting the implant, is foreseen. The choice of poly-silicon as biasing technique is mainly due to its established radiation resistance, and it relies on the capability of producers in defining the resistance value by means of controlled doping by implantation or diffusion. The resistor value is requested to be 1.5 ± 0.5 MΩ.
The strips are AC coupled using integrated coupling capacitors. The manufacturers have implemented multiple thin layers of SiO_2 and Si_3N_4. A thicker oxide fills the interstrip gap.
Two rows of AC pads are used at the edges of the strips on each side of the detector to allow for bonding and testing. An example of a wedge shaped sensor design is shown in Fig. 3.

A series of reference marks is drawn in the n^+ implanted region, for assembling and mechanical survey purposes. Every sensor is identified by a binary code created by scratching dedicated pads in the non-active region.

The CMS tracker sensors are foreseen in 15 different geometries: two rectangular detectors for the TIB (see dimensions in Tab.1), two for the TOB (Tab.2), and eleven wedge-shaped detectors for the TID and the TEC (Tab.3).

The strip pitch varies from the inner to the outer layers. The pitch is tuned in order to match the electronic modularity of 256 channels. Moreover the range of the chosen strip pitch is also driven by two particle separation and the achievable two-hit resolution, whereas the range of strip lengths is driven by minimum bias event occupancy and noise levels.
The wedge detectors measuring the ϕ-coordinate are designed, ring by ring, with the strips pointing to the interaction point. This results in a constant angular pitch in each ring and in a slightly varying linear pitch along the sensor.

Type	Length [mm]	Height [mm]	Pitch [μm]	Strips	multipl.
IB1	63.3	119.0	80	768	1536
IB2	63.3	119.0	120	512	1188

Table 1: Inner Barrel thin sensors, geometrical dimensions and multiplicities: IB1 will be mounted on 768 double-sided modules in the two inner layers of the TIB, IB2 in 1188 single modules in the two outer layers.

Type	Length [mm]	Height [mm]	Pitch [μm]	Strips	multipl.
OB1	96.4	94.4	122	768	3360
OB2	96.4	94.4	183	512	7056

Table 2: Outer Barrel thick sensors, geometrical dimensions and multiplicities: OB1 will be mounted on 1680 single-sided modules in the layers 5 and 6 of the TOB, OB2 in the inner TOB layers (1-4) in single and double modules. All the TOB detectors are composed of two daisy-chained sensors.

Thick sensors will be supplied to the Tracker Collaboration by STM[1)] and thin sensors by HPK[2)]. They differ in

[1)] ST Microelectronics, Catania, Italy

[2)] Hamamatsu Photonics K.K., Hamamatsu-City, Japan

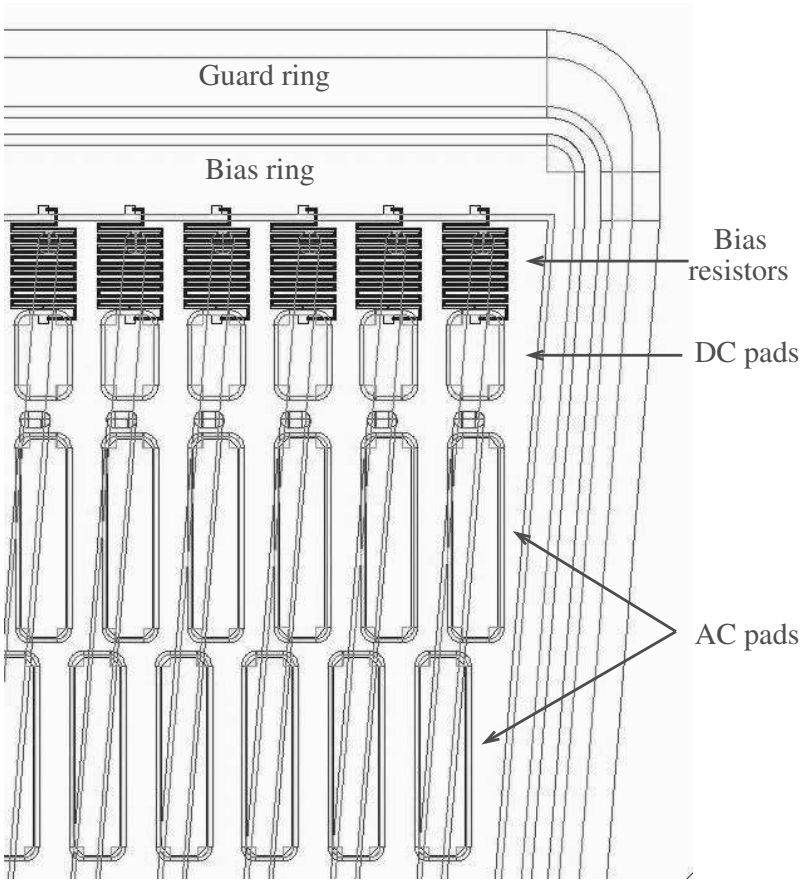

Figure 3: View of the active region edge of a wedge-shaped detector for ring 3.

Type	Length 1 [mm]	Length 2 [mm]	Height [mm]	Pitch [μm]	Strips	multipl.
W1 TEC	64.6	87.9	87.2	81-112	768	288
W1 TID	63.6	93.8	112.9	80.5-119	768	288
W2	112.2	112.2	90.2	113-143	768	864
W3	64.9	83.0	112.7	123-158	512	880
W4	59.7	73.2	117.2	113-139	512	1008
W5a	98.9	112.3	84.0	126-142	768	1440
W5b	112.5	122.8	66.0	143-156	768	1440
W6a	86.1	97.4	99.0	163-185	512	1008
W6b	97.5	107.5	87.8	185-205	512	1008
W7a	74.0	82.9	109.8	140-156	512	1440
W7b	82.9	90.8	90.8	156-172	512	1440

Table 3: Geometrical dimensions and multiplicities for thin (W1-W4) and thick (W5a-W7b) wedge sensors for TID and TEC: W1 has two different versions for TID and TEC, whereas the TID shares identical W2 and W3 sensors with the TEC. W1, W2 and W5 will be assembled in double sided modules, the other geometries in single-sided modules.

the distance from the active region to the sensor edge, calculated on the basis of the wafer thickness, and for slight variations in the dimensions of the bias and guard ring, of the DC and AC pads, of the bias resistors, in the shape of the reference marks and of the openings in the passivation layer.
Details of the process are under the provider responsibility and hence can vary for thin and thick sensors, so long as the fabrication process is kept constant for all the production.

2.2 Test structures

The wafer hosts additional devices beyond the main detector, designed to monitor the stability of the production process (see section 4). A standard set of nine structures is placed inside the fiducial region (called half-moon because of its shape) and it is shown in Fig. 4. The design is identical for all sensor geometries and for all suppliers. From left to right it is composed of:

- Ts-Cap, an array of 26 AC coupled strips, characterised by the same dielectric composition of the main sensor but with a direct connection to the bias ring, without bias resistors.
- Sheet, composed of nine superficial structures, to measure sheet resistance: three implant strips, three aluminum strips, three poly-silicon resistors, all lying directly on the n-doped bulk.
- GCD, a set of four Gate Controlled Diodes, two circle-shaped and two square-shaped.
- Cap-Ts-AC, a device built of nine strips with the same structure of the main sensor. The three external strips on each side are connected through their metallization, to facilitate their grounding.
- The mini-sensor, a small-size replica of the main detector. It has a rectangular shape with 192 strips at a pitch of 120 μm. The second rows of pads is displaced by 2 mm with respect to the bias-ring, in order to perform bonding tests.
- Cap-Ts-DC, similar to Cap-Ts-AC, except for the fact that the strips are not connected to the bias ring, either directly or through a bias resistor. In addition the dielectric layer is missing in the strips and the p^+ implant can be contacted all over their length.
- Diode, a simple diode, surrounded by a guard ring
- Two MOS devices. For both the MOS devices included in the HPK structures and for the first MOS in STM wafers, the dielectric composition corresponds to the thick oxide layer that is present in the interstrip region in the main detector. In the second STM MOS the dielectric layer follows the structure of the decoupling capacitance in the detector strips. It is hence made of thin layers of SiO_2 and Si_3N_4.

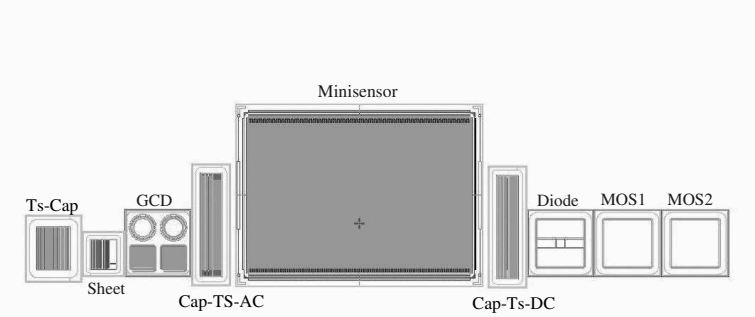

Figure 4: The standard half-moon containing nine test structures.

3 Sensor Quality Control

The strategy for the quality control of the sensor production foresees several phases, some of which have already been completed. The first step was to agree with vendors on a comprehensive list of tests that sensors must pass before being shipped to CERN. The second one has been to develop measurement set-ups in four Quality Test Centres (Karlsruhe, Perugia, Pisa and Vienna) where sensors will be tested by CMS.

The sensor production is divided into two stages. The first is a pre-series and amounts to 5% of the whole production. During pre-series all sensors delivered will be tested. Once these have been qualified, it is the responsibility of the vendor to ensure that no changes in the processing or in the substrate material properties, which could compromise the sensor performances occur during production. The pre-series has been delivered end of 2002 and the results and experience presented in this paper are based on these pre-series sensors. In the last phase -the full production- we will continue to monitor the quality on a sample basis (5 - 10 %) only.

In order to ensure the quality of the sensors used for the module construction, we have defined a detailed list of tests to be done by QTC. They can be divided in two categories: optical inspection and electrical characterization. Hereafter a description of each test and of relative acceptance criteria is given.

3.1 Optical inspection

The optical inspection consists in a survey by eye, an inspection under a microscope and a metrology of a few characteristic distances.

In the survey by eye the packaging is checked for damage and the sensor is checked for big scratches, anomalous coloration or any evident defect. Afterwards, the sensor undergoes a detailed inspection of its edges under a microscope. This is because the edges are a zone of potential fragility during some operations (like cutting, packaging and manipulation in general) where breaks can occur. If the damage is large (the limit set for the CMS sensor is 40 μm), there can be an injection of charge and a considerable increase of the leakage current or an instability in the electrical behaviour of the sensor. Finally, the precision of the cut is checked, measuring the distance between the edge and the active area at eight points near the four corners of the sensor. The precision required in the cut is $\pm$20 μm.

3.2 Electrical characterization

The equipment required to perform the electrical characterization consists in a computer controlled set-up with a probe-station, a high voltage supply, an electrometer, a capacitance meter and a switching device.

Two main goals drove the design of the set-up for the electrical characterization. Firstly, to automate and speed up the measurements as much as possible; secondly, to touch sensors with probes as little as possible. In order to achieve the first goal, two different strategies have been adopted. The probe-stations in Perugia and Pisa are equipped with an automatic loader and pattern recognition software, that permits testing of sensors 24 hours per day without human intervention (up to 25 sensors can be loaded in a single cassette). These probe-stations also use probe-cards, that permit to contact and test several strips (up to 29) at once, but need to ramp up and down the bias voltage when moving from one group of strips to another one. Fig. 5 shows the probe-station used in Perugia. The probe-stations in Karlsruhe and Vienna (without automatic loader), use single needles to contact the strips and one needle is attached to the chuck to contact the bias ring; in that way it is not necessary to ramp up and down the voltage during the measurement of every strip. Both systems make a complete electrical test of a sensor in 3-4 hours (depending on the number of strips). The second goal has been reached by using a switching device, to which all instruments are connected. This permits us to perform all measurements on every strip in sequence, so that each strip is contacted only once.

All parameters needed to perform the tests and the analysis are stored in an input file, which is centrally maintained at the Vienna QTC and, in case of agreed changes, re-distributed to all QTCs. The results of a quality control test on a sensor is written into a XML file which is inserted into the CMS Tracker database.

The electrical characterization consists of two global (IV, CV) and four strip-by-strip (I_{strip}, R_{poly}, I_{diel}, C_{AC}) tests. The electrical characterization is performed in a clean room with controlled temperature and humidity.

- IV: Measurement of the total leakage current of the sensor from 0 to 550 V reverse bias. The current is measured between the back-plane and bias-line, keeping the guard-ring floating, in steps of 5V/s. The leakage current must fulfill three criteria: 1) maximum value at 300 V less than 5 μA, 2) maximum value at 450 V less than 10 μA, 3) maximum increase in the range 450 V - 550 V less than 10 μA.

- CV: Measurement of the total capacitance of the sensor from 0 to 350 V reverse bias. The capacitance is measured between the back-plane and bias-line, keeping the guard-ring floating, in step of 5V/s, at a frequency of 1 kHz. From this measurement it is possible to extract the depletion voltage of the sensor and to check its thickness.

Strip-by-strip tests are performed at a bias voltage of 400 V, and are aimed at the identification of defective strips.

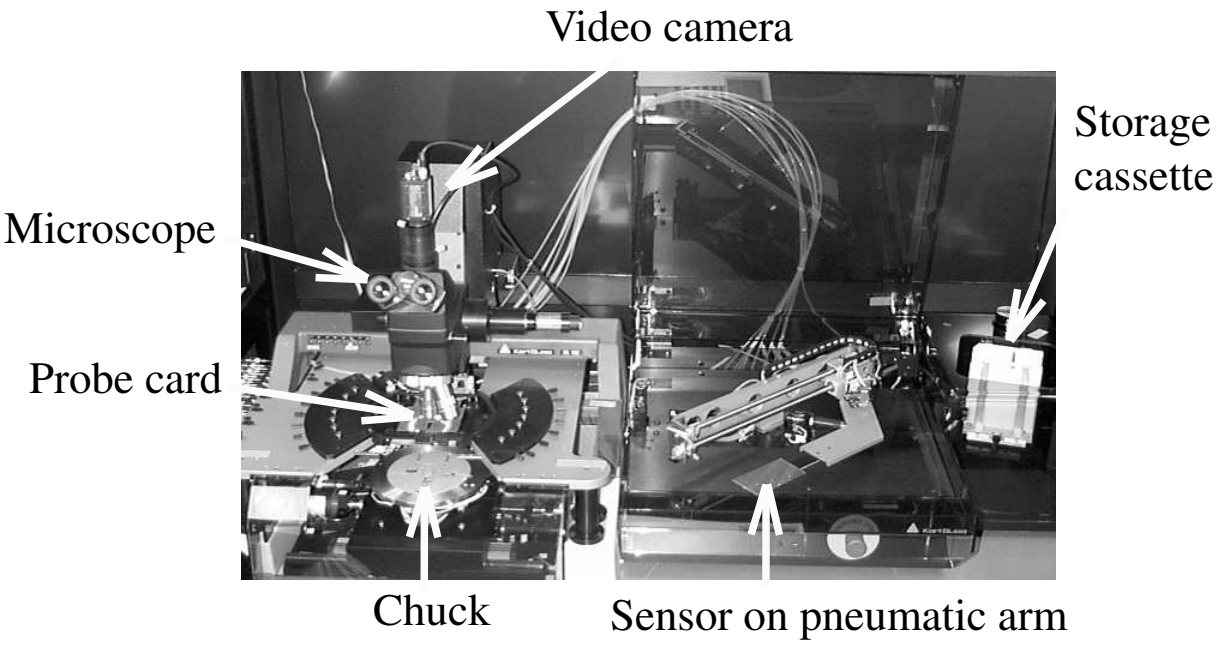

Figure 5: Automatic probe-station with loader

The limit on the total number of defective strips per sensor is 1 %. All four strip-by-strip tests are performed in the same scan, by contacting DC and AC pads simultaneously and by switching between different measurements.

- I_{strip}: The leakage current of each strip is measured in order to identify leaky (i.e. noisy) strips. The limit on the strip current is 100 nA.

- R_{poly}: The value of each poly-silicon resistor connecting strips to the bias line is measured. We require that each resistor value is 1.5 $\pm$ 0.5 MΩ. Within a single sensor we also require a uniformity of $\pm$0.3 MΩ with respect to the average value of R_{poly} for that sensor.

- I_{diel}: This measurement is devoted to the identification of pinholes. We apply 10 V at the coupling capacitor of each strip and measure the current across it. When the capacitor is good the current equals the noise of the set-up (of the order of a pA). If I_{diel} exceeds 1 nA, the strip is classified as defective.

- C_{AC}: The value of the coupling capacitor for each strip is measured. This is again a check for pinholes and monitors the uniformity of the oxide layer. The measurement is performed in such a way that it can also detect metal shorts between neighboring strips, in fact the capacitance is measured between two adjacent DC pads shorted together and the corresponding central AC pad. In that way shorted strips are measured as two capacitors in parallel and the resulting value is twice the correct one. The measurement is performed at a frequency of 100 Hz.

Up to now about 1200 sensors of different types have been delivered by the two companies (STM and HPK) and were tested in the four QTCs. The aim of this paper is not to give a complete summary of test results, so just a few plots of the most significant results will be showed. Fig. 6 show the distribution of the total current measured at 450 V for all sensors tested up to now. Despite the differences in geometry, thickness and resistivity, all sensors are produced from 6" wafers and are of similar area, so that their total current can be roughly compared. The plot shows that 95 % of sensors fulfil the requirement of a total current at 450 V lower than 10 μA which is equivalent to 100 - 150 nA/cm^2 depending on the sensor surface. Fig. 7 and Fig. 8 show the distribution of depletion voltage for thick and thin sensors respectively. The requirement on resistivity (3.5 - 7.5 kΩ cm, for thick sensors and 1.5 - 3.0 kΩ cm, for thin sensors), the thickness of wafers, the pitch and the ratio of width/pitch for different types are such that every sensor should deplete between 100 and 300 V. The peak in Fig. 8 at small depletion voltage, is due to the first batches produced on 'non-standard' material in the pre-production phase. Finally, Fig. 9 and 10 show the number of pinholes detected on sensors with 512 strips and 768 strips respectively. The requirement that no sensor has more than 1 % of strips with a pinhole is globally satisfied by 96 % of sensors.

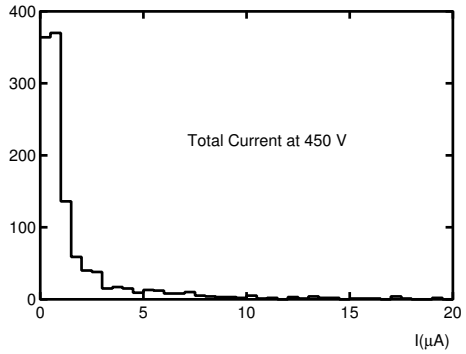

Figure 6: Total current at 450 V

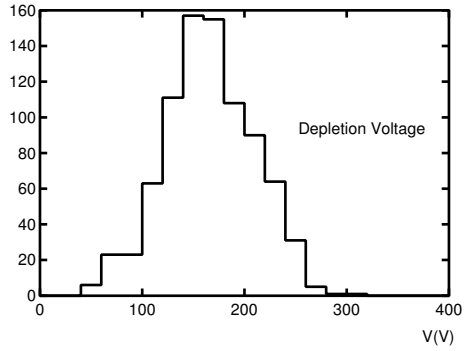

Figure 7: Depletion voltage for thick sensors

4 Process Control

The main purpose of the Process Control is to ensure a constant quality throughout the production and to detect any problem as soon as possible. This control is based on the characterization of the test structures which are produced on the same wafers together with the sensors. During the pre-production, most of the test structures will be measured in contrast to only 5% during the mass production. Ten different measurements on eight different structures are carried out in Florence, Strasbourg and Vienna.

In addition longtime tests are done using full sensors in Strasbourg and Vienna.

4.1 Measurements on dedicated test structures

The process control on the test structures consists of the following measurements (see Fig. 4 in section 2): CV on the MOS devices, CV on the diode, interstrip resistance between a central strip and its two first neighbours on Cap-Ts-DC, IV on the mini-sensor, interstrip capacitance between a central strip and its two closer neighbours on

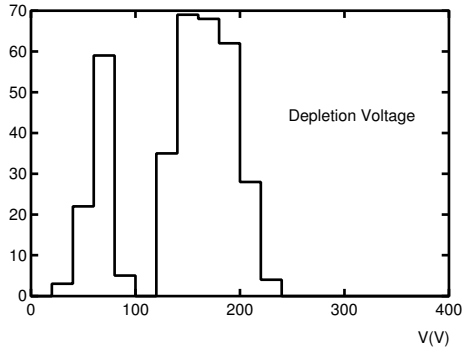

Figure 8: Depletion voltage for thin sensors

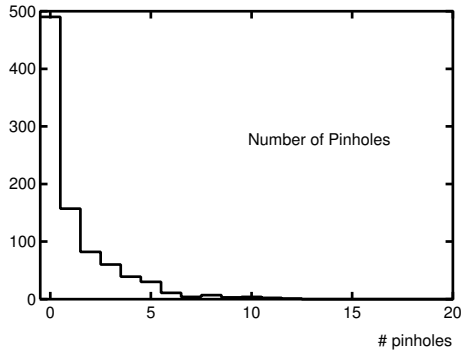

Figure 9: Number of pinholes for 512 strips sensors

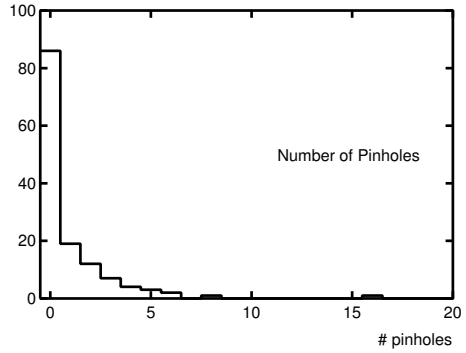

Figure 10: Number of pinholes for 768 strips sensors

Cap-Ts-AC, IV on one of the square gate controlled diode, the set of resistances of poly, aluminum and p^+ on the sheet structure, six coupling capacitances in Ts-Cap, and finally the breakdown voltage of the decoupling capacitor oxide.

In the following the set up, the common software and finally the measurements together with the results from the pre-series will be described.

4.1.1 The process control set-up

To contact all 49 pads on the test structure a probecard was designed. The probecard output is connected via a switching matrix to the four measurement devices (LCR-meter, ammeter and two voltage sources). In Fig. 11 is shown a schematic of the electrical layout. To avoid possible bad contacts, the probes have been doubled each time it seemed useful. As we are using mostly common equipment in the three labs, a common software has also been adopted based on Labview and made of three components: acquisition, analysis and database interface.

The acquisition part manages the ten measurements. The sequence of the measurements is done automatically but if needed, a single measurement can also be done manually. An emergency stop is implemented and if any current compliance is reached, the measurement is stopped.

After some measurements are performed, an analysis is needed to extract relevant parameters; This is the case for CV on MOS, CV on diode and IV on gate controlled diode. The basic tool for the analysis is the linear fit, which is used to find kinks between different linear regions.

An example of a CV on MOS is shown in Fig. 12. We first check the maximum capacitance. The flat band voltage V_{fb} is then obtained by fitting the position of the sharp drop of the capacitance value.

The IV curve on the gate controlled diode usually shows three regions as shown in Fig. 13. Starting to decrease the gate voltage from the plateau of electrons accumulated under the gate, an increase of the current from the flat band voltage can be seen, corresponding to a growing depletion. There is then a plateau of maximum current (full depletion under the gate) and finally, at a voltage value (V_{bias} + V_{fb}), a sharp decrease down to low values corresponding to the inversion regime. The surface current is directly extracted from the height difference between

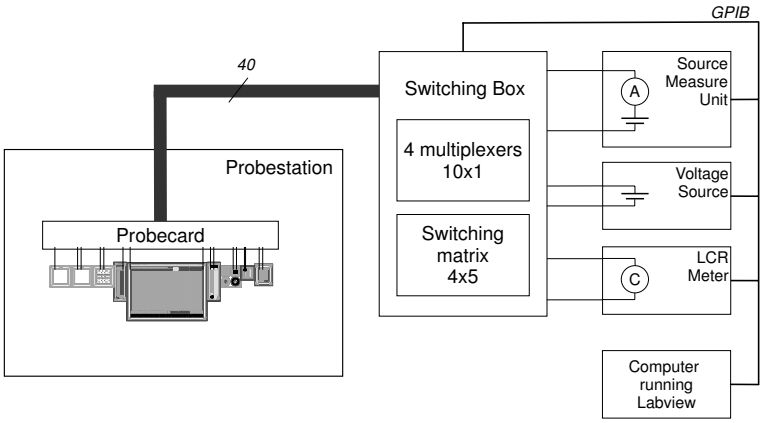

Figure 11: Schematic of the common set up

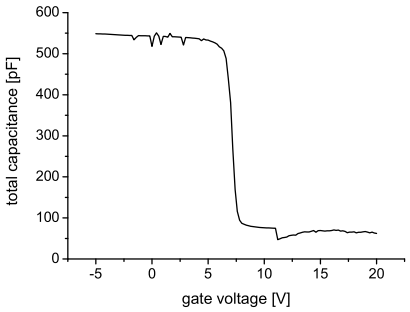

Figure 12: Result of a CV on MOS

the full depletion and the inversion plateau. The sharp decrease voltage identifies the flat band voltage by subtracting the bias voltage and can be crosschecked with the CV on MOS study. From the surface current, the surface recombination velocity is finally deduced. This velocity characterizes the quality of the silicon/insulator interface and consequently the quality of the passivation between the strips.

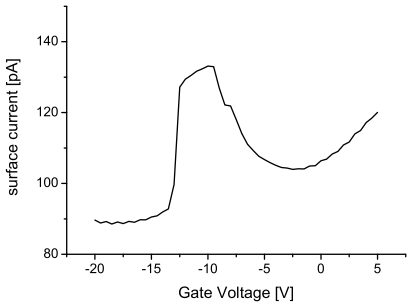

Figure 13: IV plot of the gate controlled diode

All the measurements done are stored in the tracker database. The same procedure of the QTC is adopted. All the parameters needed for the set of measurements comes from an input file. At the end of the measurement series, the output file is produced in XML format.

4.1.2 First results from the pre-production

The PQC tested 269 standard half-moons of the STM pre-series and 18 standard half-moons from HPK. The results of the pre-production measurements are shown in Fig. 14 and Fig. 15. The average values of the relevant PQC

variables are listed in Tab.4.

About 84 % of the STM batches have been accepted. The main problem found in the rejected test-structures consisted of a value of the flatband voltage exceeding our specifications. Following our request, STM has agreed to implement the measurement of the flat band voltage as a standard check before delivering the sensors.

The whole HPK pre-production has been accepted.

Type of measurement	HPK	STM
C_{ac}	23.0 pF	17.2 pF
$V_{break\ diel}$	$>$ 169 V	$>$ 195 V
ρ_{Alu}	24.4 mΩ/square	26.6 mΩ/square
ρ_{p^+}	118 Ω/square	181 Ω/square
R_{poly}	1.66 MΩ	1.33 MΩ
$I_{surface}$	46.4 pA	43.7 pA
C_{int}	0.48 pF	0.76 pF
$V_{breakdown}$	$>$ 700 V	$>$ 689 V
R_{int}	$>$ 56 GΩ	$>$ 96 GΩ
V_{depl}	125 V	134 V
V_{fb}	1.5 V	7.73 V

Table 4: Average values of the results of PQC measurements: coupling capacitance (C_{ac}) and breakdown voltage for the dielectric layer ($V_{break\ diel}$), resistivity of the p^+ implant and of the aluminium layer (ρ_{p^+} and ρ_{Alu}), value of the poly-silicon resistors (R_{poly}), surface current ($I_{surface}$), interstrip capacitance (C_{int}), breakdown voltage of the mini-sensor ($V_{breakdown}$), interstrip resistance (R_{int}), depletion voltage (V_{depl}) and Flat Band Voltage measured on the MOS (V_{fb}).

4.2 Longtime test of sensors

One of the tests of the CMS process control is a long term stability test at room temperature. This test is done on a small, but representative sample of all sensors delivered by the two suppliers. The study of the long term stability of the sensors is necessary, because once the detector is installed in the experiment, the access will be very limited. Therefore we must ensure that the dark current of the sensors is below the specified value and stable in time.

Two measurement set ups were installed in Strasbourg and Vienna to perform this test.

4.2.1 Longtime set up

A light-tight box contains ten plates with a conducting rubber surface, mounted individually on moving slides. The sensors are placed on these plates which also provide the backplane contact. The bias ring of each sensor is connected by wire bonding to a wiring pad connecting the measuring instruments. At the top and the bottom of the box combined temperature and humidity sensors are placed. These sensors are connected to a home-made system, which reports the measured values to a computer by a serial connection. The humidity is controlled by blowing dry air or nitrogen gas into the box. The gas flow is switched by an electromagnetic valve, which is also driven by the computer in order to keep the relative humidity between 10% and 30%.

A reverse bias voltage of 400 V is applied to each sensor with a resistor of $470\,\mathrm{k}\Omega$ connected in series. The voltage drop across these resistors is measured by a scanning voltmeter or a switching system.

The experiment is controlled by a computer running a Labview application program. The program reads the sensor currents derived from the voltage drops, the temperature and the humidity from the instruments every minute, and displays the data online. After the measurement is finished an XML file for each tested sensor is created to be inserted into the CMS Tracker database.

4.2.2 Results from the longtime tests

A typical long term measurement lasts about five days. During that period the sensor dark currents are recorded. To quantify the results of each sensor, we defined a stability parameter as the standard deviation of the sensors current with respect to the mean value of the current over the whole measurement time. Accordingly, a lower

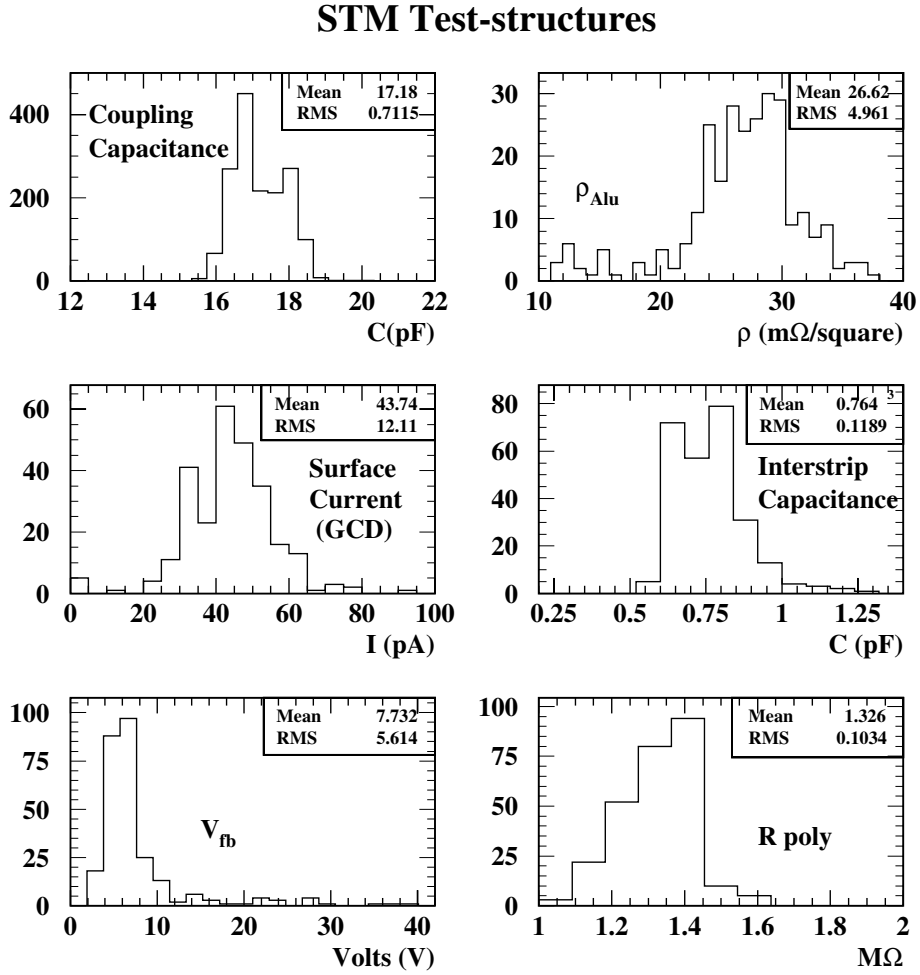

Figure 14: Results of PQC measurements on STM pre-series test-structures: on the top left plot the distribution of the coupling capacitance, on top right the aluminium resistivity, on middle left the surface current, on middle right the interstrip capacitance, on bottom left the Flat Band Voltage and on bottom right the poly-silicon resistor.

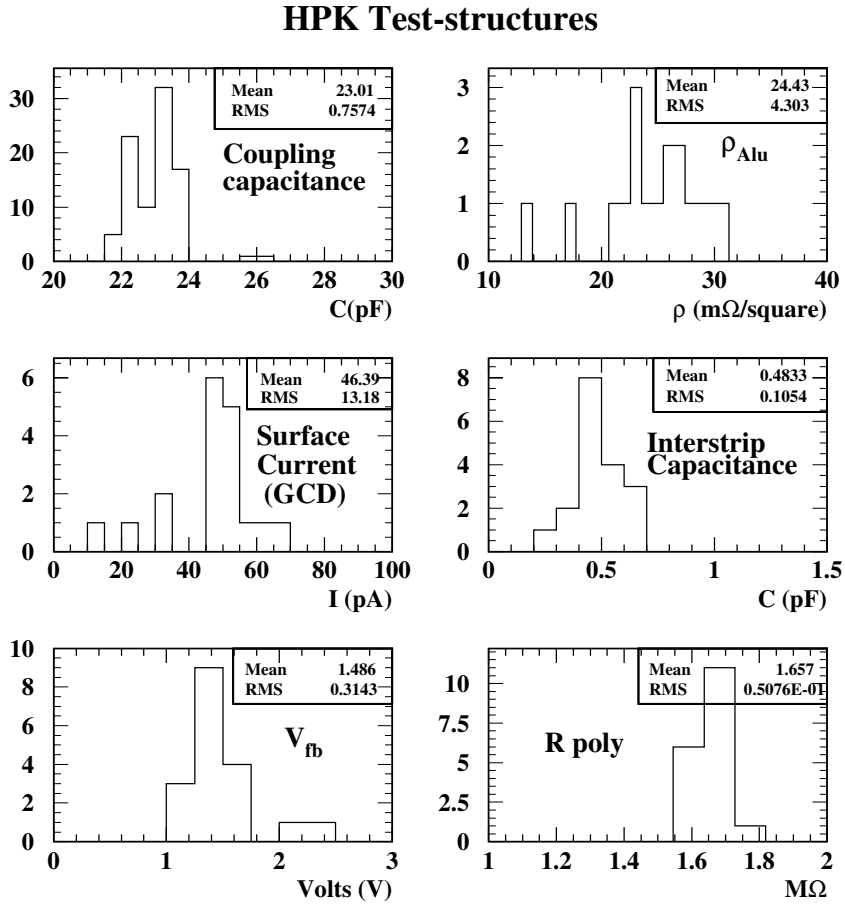

Figure 15: Results of PQC measurements on HPK pre-series test-structures: on the top left plot the distribution of the coupling capacitance, on top right the aluminium resistivity, on middle left the surface current, on middle right the interstrip capacitance, on bottom left the Flat Band Voltage and on bottom right the poly-silicon resistor.

value corresponds to a more stable sensor behavior. Histograms of the results obtained for HPK sensors and for STM sensors are shown in Fig. 16. Up to now, 136 sensors from both companies have been analyzed. With one exception, all these sensors were very stable. Their dark currents are far below the specified limit of $10\,\mu$A at 400 V.

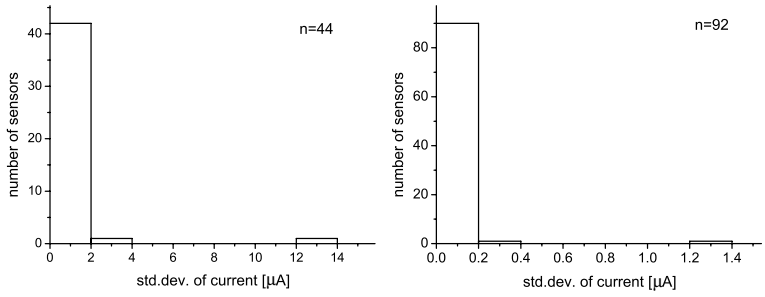

Figure 16: Distribution of the standard deviation of the HPK sensor currents (left) and the STM sensor currents (right) with respect to their average. Notice the different scales in the abscissa.

5 Irradiation Quality Control

To ensure the required radiation hardness of the sensors irradiation experiments using neutrons and protons are performed. As this is a destructive test mainly test structures and only a small number of sensors (about 1%) will be selected for these tests plus about 5% of dedicated mini-sensors processed on the remaining halfmoons of the wafers. The microstrip silicon sensors and test structures for the CMS tracker are electrically tested before and after the irradiation. Before being measured, they were annealed for 80 minutes in an oven kept at $60°C$. These tests are mainly electrical measurements, such as the CV and the IV characteristics, the evaluations of the interstrip resistances and capacitances, measurement of the biasing resistors and pinhole check (dielectric current and coupling capacitances).

5.1 Irradiation with Neutrons

Over the ten years of LHC operations, sensors will receive a fluence equivalent to 1.6 10^{14} neutrons (1 MeV) per square cm. The test aims to check that the sensors would be able to sustain this flux without degradation of their performances. To reach such a high fluence in a reasonable time, an intense fast neutron beam was developed based on the reaction ^{9}Be + d $\rightarrow$ n + ^{10}B. The Louvain-la-Neuve isochronous cyclotron delivers a high intensity deuteron beam of 50 MeV on a 1 cm thick, 2 cm diameter beryllium target. To harden the neutron energy spectrum we added a special shielding made of 1 cm thick polystyrene, 1 mm of cadmium and 1 mm of lead just after the thin stainless steel window of the beam pipe. This also helps to reduce the contamination of the beam by charged particles. Since the neutron distribution across the spot is non-uniform, there is a compromise to be made between the size of the sample to be irradiated, the distance to the production target, the uniformity of the neutron beam spot, and the total time to reach a given fluence. Typically, to produce a beam spot on the sensors with a flux distribution uniform to within 80 % (i.e. the beam flux across the spot varies by 20 % between the beam axis and the edges of the spot), a sample with a diameter of 6 cm has to be placed at about 50 cm from the target. At the minimum distance from the target (5 mm) the neutron beam spot is about 20 mm.

To determine the fluence achieved during irradiation we used the following equipment: a floating current digitizer is used to determine the integrated deuteron beam current on target (on-line monitor); alanine dosimeters are systematically placed with each silicon device to evaluate irradiation uniformity. We also used several activation foils to look at the beam energy spectrum, and standard silicon pad diodes are also irradiated to compare their leakage current and depletion voltage with literature (e.g. [4]).

5.1.1 Description of the set up for neutron irradiation

The set up reproduces as closely as possible the LHC environment. During the neutron irradiations sensors and structures are biased and maintained at low temperature (-10°C) in a dry air atmosphere. During irradiation, we monitor the temperature and the deuteron beam current. We also monitor the applied bias voltage and the current drawn by the test structures from the bias supplies via a CAENet control bus, and from the sensors by the use of analog outputs from the HV supplies. The software is also used to control the various power supplies.

The sensors or test structures are supported by specially prepared polycarbonate frames (Lexan) 3 mm thick. The frames have an opening of 12 cm: this is large enough to ensure a uniform fluence of the elements to be tested (diodes and mini-sensors on the standard test structure). The electrical contacts to the bias line are done using wire bonds. Several such frames can be stacked for the irradiation of as many as ten halfmoons (or five full size sensors). According to this scheme, the fluence variation across the different plates is below 10 % with respect to the fluence of the central layer (set to be the nominal LHC fluence).

The set up for measuring the structures before and after the irradiation uses a semi-automatic probe station. Its air-tight enclosure is fed with dry air: the relative humidity inside the enclosure is about 1-2 % corresponding to a dew point of about -40°C. The chuck can be regulated with Peltier elements to -10°C corresponding to the operating conditions of the CMS tracker. To connect the structures with the instruments, a set of five needles is arranged around the chuck. Two voltage sources, a switching device, a LCR and an electrometer are used to perform the tests. A LabView program, running on a separate PC, controls everything from the probe station to the temperature of the chuck. The test parameters are easily modified by the use of global variables. After irradiation, results are compiled in a XML file to be put into the Tracker database.

5.1.2 Results of first neutron irradiations

The results presented here were obtained with sensors and test structures irradiated up to $2.1 \cdot 10^{14} \frac{n_{eq}}{cm^2}$. Apart from annealing and test periods, the devices were kept at low temperature in a refrigerator.

After irradiation, the thin sensors (HPK) as well as the thick sensors (STM) showed no significant changes in the strip parameters, although it is sometimes observed that the coupling capacitances show a slight decrease of about 1 %.

The total leakage current between the backplane and the bias ring, has been measured as a function of the reverse bias voltage from 0 to 800 V. As expected, we notice that the leakage current is much higher after irradiation and reaches saturation at around 600 V. The devices show a leakage current below the acceptance criteria of $\alpha \leq 4.5$ 10^{-17} A/cm, if tested after 80 minutes of annealing at 60°C.

To extract the depletion voltage, we measured the backplane capacitance as a function of the reverse bias voltage from 0 to 800 V. We have compared the results before and after neutron irradiation. As the capacitance at the depletion voltage decreases after irradiation, the depletion voltage itself increases. The obtained depletion voltages are all below the permitted maximum value of 300 V after beneficial annealing.

5.2 Irradiation with Protons

Irradiations with protons take place at the isochrone cyclotron of the Forschungszentrum Karlsruhe. It provides 26 MeV protons at beam currents of up to 2 μA. This allows to irradiate a 100 cm^2 sensor up to $1 \cdot 10^{14} \frac{p}{cm^2}$ within 20 min using a scanning device. To ensure the desired fluence (0.35 and $1.6 \cdot 10^{14} \frac{n_{eq}}{cm^2}$ for outer and inner barrel respectively [3]) an online current control and calibrated nickel foil dosimetry for integral measurement is used.

5.2.1 Description of the set up for proton irradiation

The sensors and test structures are arranged in a cold box where a maximum number of three frames can be fitted. One frame can contain up to four test structures or one sensor. Each structure is clamped between a metal foil on the back and a conductive rubber strip on the front (Fig. 17), which sets the AC pads and the bias ring to ground as in the experiment, where the read-out chip grounds the AC pads.

5.2.2 Results of first proton irradiations

One outer barrel sensor from STM, one wedge shaped sensor from HPK and several additional test structures were tested in a first irradiation.

Both sensors were biased with 1 V and several voltages were used for the test structures (0 V, 1 V, 12 V, 100 V). The value of 1 V is the estimated potential drop over the oxide after ten years of LHC operation. Since the development of oxide charges depends on the electric field, the structures are biased with at minimum 1 V. During irradiation they are kept below -10°C to avoid annealing and thermal runaway due to the higher leakage current.
The irradiation was performed up to $2.6 \cdot 10^{14} \frac{n_{eq}}{cm^2}$ and $0.9 \cdot 10^{14} \frac{n_{eq}}{cm^2}$ for the HPK and STM stack respectively

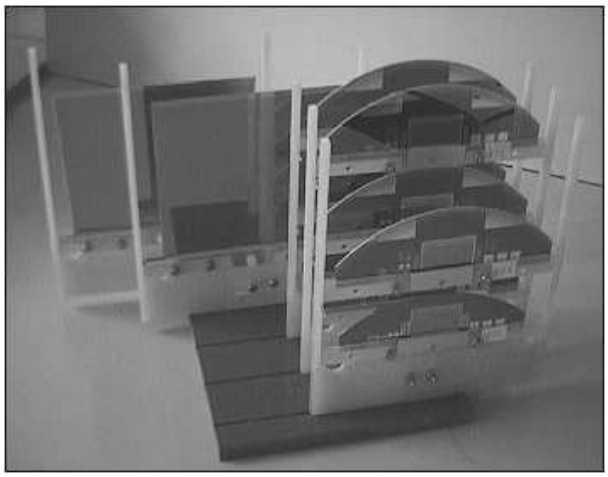

Figure 17: Sensors and test structures mounted in frames. Electrical contact was made by conductive rubber on the front.

(derived from leakage current measurements).
After irradiation the structures are stored at -18°C to stop all annealing processes.

Strip values (such as coupling capacitance, bias resistance and interstrip capacitance) showed no changes after irradiation. The leakage current of the strips increased according to the expected rise of the total leakage current. For the measured values one can extrapolate the maximum leakage current for 500 μm sensors to be 280 μA for a large outer barrel sensor (Fig. 18).

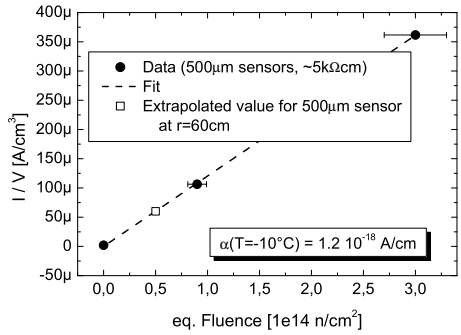

Figure 18: Specific leakage currents and extrapolated value for 500 μm sensors with maximal fluence for this material.

The resulting full depletion voltages match the calculated voltages from the 'Hamburg model' using close to mean values from reference [4]. From these values a full depletion voltage for 500 μm sensors after ten years of LHC operation ($0.5 \cdot 10^{14} \frac{n_{eq}}{cm^2}$) is estimated to about 280 V (Fig. 19).

Since there are identical minisensors on every test structure, independent of the sensor geometry, it is possible to measure all parameters of interest on several strips on the mini-sensors, thus achieving a good statistical significance for the measurements.

6 Summary

We have presented the design of the silicon sensors for the CMS tracker. The design follows several years of research and development together with silicon sensor manufacturers. The performances of the prototypes have proven that the design is safe and robust. Nevertheless CMS has developed an elaborate quality assurance procedure to assure the quality of all sensors delivered during the production period. The seven institutes involved in these tests have developed fully automatic set-ups to cope with the large number of sensors.

The CMS test centres for the Quality, the Process and the Irradiation Controls have tested more than a thousand sensors and test structures during the pre-series production. About 10% of the sensors received in 2002 were

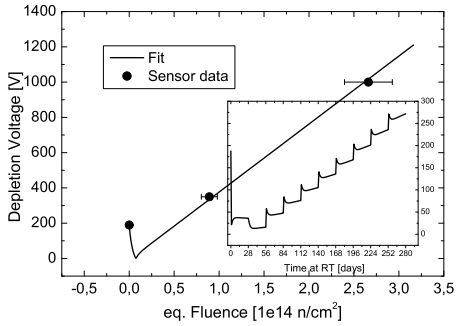

Figure 19: Full depletion voltages fitted with Hamburg model and calculation for 10 years LHC with 28 days at room temperature each year.

measured with values outside the technical specifications. These non-compliances were discussed with the supplier and were subsequently solved.

The full series-production of more than 24000 sensors has started and the first sensors arrived towards the end of 2002.

7 Acknowledgment

We would like to thank D.Gagliardi (Pisa) for the technical support and C. Hoffmann (Strasbourg), C. Menge (Karlsruhe), M. Oberegger (Vienna) and T. Punz (Karlsruhe) for their help obtaining the measurement results.

References

[1] S. Braibant et al., Investigation of design parameters for radiation hard silicon microstrip detectors, Nucl. Instrum. Methods A, 485 (2002) 343-361

[2] The CMS All-Silicon Tracker - Strategies to ensure a high quality and radiation hard Silicon Detector, Frank Hartmann on behalf of the CMS Silicon Tracker Collaboration, Nucl. Instrum. Methods A 478 (2002)

[3] CMS Tracker TDR, CERN/LHCC 98-6 CMS TDR 5 (1998)

[4] M. Moll, Ph.D. Thesis, DESY-THESIS-1999-040 (1999)